

The Journal of Advanced Undergraduate Physics Laboratory Investigations, JAUPLI-B

Volume 3

Article 1

2014

Modeling the Motion of a Volleyball with Spin

Julian Ricardo
Amherst College

Follow this and additional works at: <https://digitalshowcase.lynchburg.edu/jaupli-b>



Part of the [Engineering Commons](#), and the [Engineering Physics Commons](#)

Recommended Citation

Ricardo, Julian (2014) "Modeling the Motion of a Volleyball with Spin," *The Journal of Advanced Undergraduate Physics Laboratory Investigations, JAUPLI-B*: Vol. 3 , Article 1.

Available at: <https://digitalshowcase.lynchburg.edu/jaupli-b/vol3/iss1/1>

This Article is brought to you for free and open access by the Journals at Digital Showcase @ University of Lynchburg. It has been accepted for inclusion in The Journal of Advanced Undergraduate Physics Laboratory Investigations, JAUPLI-B by an authorized editor of Digital Showcase @ University of Lynchburg. For more information, please contact digitalshowcase@lynchburg.edu.

Modeling the Motion of a Volleyball with Spin

Julian Ricardo*

*Department of Physics, Amherst College,
Amherst, MA 01002-5000 USA*

(Dated: April 29, 2014)

Abstract

Though a qualitative understanding of how spin affects a ball's trajectory can be easily developed, a quantitative one is relatively difficult to hone. Additionally, although projectile motion is an extensively covered topic in introductory physics courses, friction and drag—let alone spin—receive little to no attention. Here we use a volleyball and video modeling software to compare the behavior of a non-spinning ball with one that has topspin in order to assess the accuracy of our various models incorporating drag and the Magnus effect.

INTRODUCTION

The ubiquity of spin in ball sports—whether in baseball, soccer, or tennis—illustrates its nontrivial effect on the trajectory of a ball. Compared to a non-rotating soccer ball, for example, a rotating one arcs and swerves in a manner predictable enough that players can control its potentially deceptive flight path. When soccer commentators laud a player’s ability to bend a free kick into the upper corner of the goal, they are referring to this phenomenon. Theoretically, different types of spin can be employed in any ball sport where the rotation generated significantly affects the trajectory. Even a completely non-rotating ball has its uses, hence the famously deceptive knuckleball pitch in baseball. However, while athletes often intuit how to adjust spin to determine flight path, we are interested in quantifying these effects and showing to what extent they hold at the speeds we test.

We will be modeling the motion of a volleyball in flight, once without any applied spin and once with heavy topspin, in order to assess prevailing theories regarding the effect of spin on a ball’s trajectory. In particular, we will be investigating how accurately a model of the ball’s motion incorporating the Magnus effect, a consequence of the ball’s rotation, can describe the trajectory of our ball. We ultimately compare our experimentally optimized lift coefficient, C_ℓ , related to the Magnus force, with those found in other related studies. In the end, our experimentally determined C_ℓ of 0.25(2) is of the same order of magnitude as our expected value of 0.2. As such, our results indicate that a quantitative understanding of the Magnus force and its influence on ball flight is attainable.

BACKGROUND AND THEORY

In order to quantify the trajectory of the ball, we begin by deriving the equation of motion for the ball from first principles, namely Newton’s 2nd law. We use the free-body diagram shown in Fig. 1 to derive two equations for the volleyball’s motion, one for the vertical acceleration and another for the horizontal acceleration.

The forces acting on the ball, of mass m and with acceleration \mathbf{a} , are the Earth’s gravitational force (\mathbf{F}_g), drag (\mathbf{F}_{drag}), and Magnus forces (\mathbf{F}_{mag}). Substituting into Newton’s 2nd law, we get:

$$\mathbf{F} = m\mathbf{a} = \mathbf{F}_g + \mathbf{F}_{\text{drag}} + \mathbf{F}_{\text{mag}}. \quad (1)$$

Next, we must find expressions for each of these forces.

In deriving our equation for the drag force on the ball, we begin with the

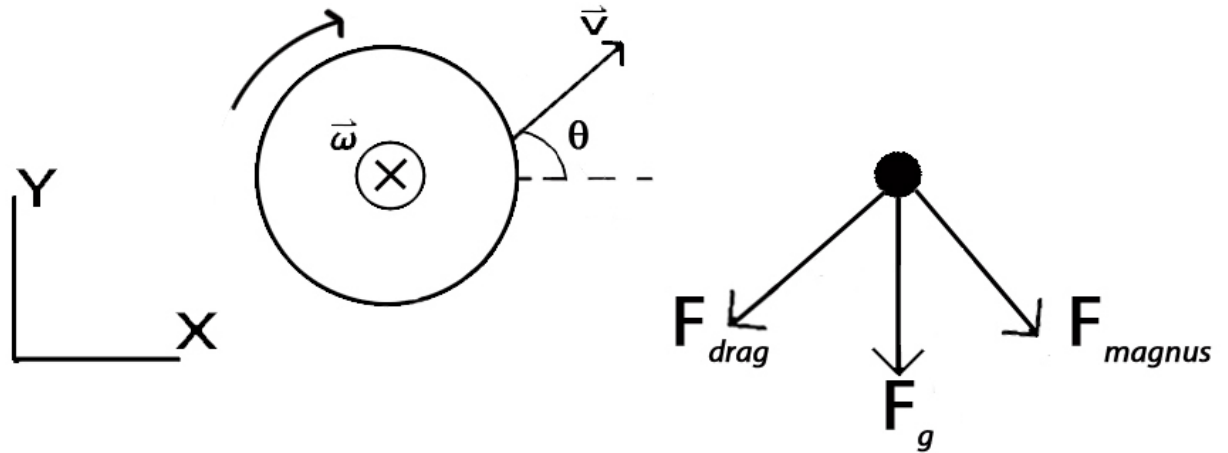


FIG. 1. The left figure shows the volleyball after being thrown with a linear velocity \mathbf{v} at an angle θ from the horizontal axis and an angular velocity $\boldsymbol{\omega}$ pointing into the page (in this case, the ball undergoes topspin). At this instant, three forces act on the ball: the gravitational force, \mathbf{F}_g , points in the negative y direction; the drag force, \mathbf{F}_{drag} , opposes the velocity; and the Magnus force, $\mathbf{F}_{\text{magnus}}$, points in the direction given by $\hat{\boldsymbol{\omega}} \times \hat{\mathbf{v}}$. The non-rotating ball has the same gravitational and drag forces acting on it, but no Magnus force.

Taylor-expanded equation for drag:

$$\mathbf{F}_{\text{drag}} = -b_0 - b_1\mathbf{v} - b_2\mathbf{v}^2 + \dots \quad (2)$$

We know, first of all, that the drag force equals zero when an object is at rest ($\mathbf{v} = 0$), so b_0 must equal zero. Additionally, we ignore all terms greater than second order — often a good approximation at low enough speeds like the ones considered here.⁸ In order to assess the relative importance of linear and quadratic drag, we must calculate the volleyball's Reynolds number using the following equation,

$$R = \frac{\rho v D}{\eta}, \quad (3)$$

where η is the viscosity of air, which we approximate as $1 \cdot 10^{-5}$ Pa·s, ρ is the density of air, which we approximate as 1 kg/m^3 , and D is the diameter of the ball, which we measure to be $0.210(5)$ m. According to estimates based on the speeds we consider, which do not exceed 6.5 m/s , R is approximately

10^5 . A typical volleyball serve, ranging in speed from 10 m/s to 30 m/s, has been found to involve a Reynolds number greater than 200,000, the same order as our calculation.⁷ Based on this very large Reynolds number, we choose to disregard linear drag in our models and, removing the subscript from b for simplicity, conclude that

$$\mathbf{F}_{\text{drag}} = -bv^2\hat{v} = -b\mathbf{v}^2. \quad (4)$$

Whereas drag results from the forces that air particles exert in the opposite direction of a ball's motion, the Magnus effect results from the asymmetric flow of air around a spinning ball. This asymmetry creates a deflecting force in the direction of $\hat{\omega} \times \hat{v}$, the unit vectors of the ball's spin axis and velocity, respectively. We express the Magnus force according to the formula used in Bray and Kerwin's 2003 work on the flight of a soccer ball in a direct free kick,

$$\mathbf{F}_{\text{mag}} = \frac{1}{2}\rho AC_\ell \hat{\omega} \times \mathbf{v}^2, \quad (5)$$

where A is the ball's cross-sectional area. C_ℓ , the dimensionless quantity introduced earlier, is related to ρ , v , and the lifting force of the air on the ball, which points perpendicular to the air flow.³ Incorporating the gravitational force, we can now use Eq. 1 to write an equation for the net force acting on the ball:

$$\mathbf{F} = -m\mathbf{g} - b\mathbf{v}^2 - \frac{1}{2}\rho AC_\ell \hat{\omega} \times \mathbf{v}^2. \quad (6)$$

With an expression for net force, we must express its horizontal and vertical components separately in order to input them into the modeling software we use. We assume that $\mathbf{F}_{\text{mag}} = 0$ for the non-rotating volleyball. When it has topspin, we cannot explicitly measure the direction of its spin axis, but we can express the horizontal and vertical components of the Magnus effect in terms of the ball's horizontal and vertical velocities using the angle θ shown in Fig 1.

We solve for the component of Eq. 6 along the x-axis first, eliminating the gravitational force since it is solely vertical:

$$\mathbf{F}_x = m\ddot{x} = \mathbf{F}_{\text{drag}_x} + \mathbf{F}_{\text{mag}_x} \quad (7)$$

$$\mathbf{F}_x = -bv_x v - \frac{1}{2m}\rho AC_\ell v_x v. \quad (8)$$

Then, after expanding the ball's speed in terms of its two Cartesian components, the equation of motion takes the final form of

$$\mathbf{F}_x = -bv_x(v_x^2 + v_y^2)^{1/2} - \frac{1}{2m}\rho AC_\ell v_x(v_x^2 + v_y^2)^{1/2} \quad (9)$$

from which we base the horizontal component of the force in our models. In the vertical direction, we must add a term for gravity:

$$\mathbf{F}_y = -mg - bv_y(v_x^2 + v_y^2)^{1/2} - \frac{1}{2}\rho AC_\ell v_y(v_x^2 + v_y^2)^{1/2}. \quad (10)$$

With our equations of motion in order, we input our equations into our video analysis and modeling software. Table I shows the force equations that we input for both of the models we consider.

	\mathbf{F}_x	\mathbf{F}_y
Non-rotating	$-bv_x(v_x^2 + v_y^2)^{1/2}$	$-mg - bv_y(v_x^2 + v_y^2)^{1/2}$
Topspin	$-bv_x(v_x^2 + v_y^2)^{1/2} - \frac{1}{2}\rho AC_\ell v_x(v_x^2 + v_y^2)^{1/2}$	$-mg - bv_y(v_x^2 + v_y^2)^{1/2} - \frac{1}{2}\rho AC_\ell v_y(v_x^2 + v_y^2)^{1/2}$

TABLE I. The equations of motion in both horizontal and vertical directions used in Tracker.

EXPERIMENTAL METHOD

In order to conduct our experiment, we need to be able to film the ball's trajectory and model it. We use a Nikon V1 camera, two light sources, a volleyball, and a meter stick. The camera records the ball's flight at 400 frames per second and is pointed perpendicularly with respect to the plane of the ball's motion. To improve visibility, the light sources illuminate the ball, which is thrown underhand against a black background. The meter stick serves as a length reference.

To model the ball's trajectory, we then analyze the video using Tracker, a modeling software made by Douglas Brown at Cabrillo College.² It allows for the comparison of real, recorded trajectories with those of modeled point masses based on a user-defined coordinate system. We begin by calibrating the length scale to be used in the program. Next, we create the ball's trajectory by selecting its position in the video frame by frame, a process that introduces considerable uncertainty — 3 cm, roughly a quarter of the ball's radius — into our measurements of the position of the ball. Lastly, we enter the equations of motion for our model using the initial conditions of the actual ball. With both trajectories overlaid on our video, we can optimize the relevant coefficients, in this case b and C_ℓ , by observing which values result in a model path that follows the ball's trajectory for the most time.

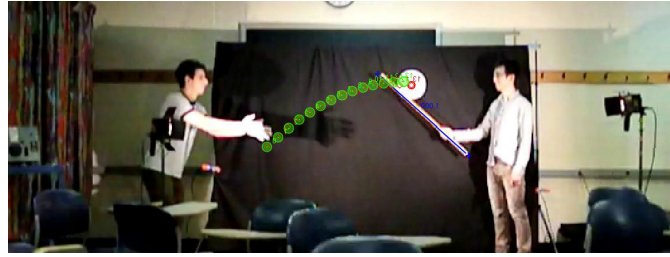


FIG. 2. Tracking and modeling the non-rotating volleyball's trajectory in Tracker software. The red dots mark the ball's path and the green, our non-rotating model's. The ball moves from left to right. The meter stick is shown for length calibration.

RESULTS AND DISCUSSION

We first conduct the experiment with a non-rotating ball and create a model of its flight using the corresponding equations in Table I. We measure the ball's radius to be 0.106(5) m, and A is therefore 0.035(7) m. Its mass is 0.175(1) kg. In Tracker, the value of b which best fits our curve (see Fig. 3) is 0.010(5) kg/m. We intend to compare this value to typical ones listed in D.J. Tritton's text on fluid dynamics, but must first convert b to the unitless drag coefficient, C_D , that Tritton uses.⁹ The two are related by

$$C_D = \frac{2b}{\rho A}.^4 \quad (11)$$

Substituting in for the three variables in the right-hand expression, we find that our converted C_D is of the same order of magnitude as those listed in Tritton for various balls, concluding that our value of b is therefore reasonable.

The uncertainties inherent in demarcating the position of the volleyball's center of mass in Tracker are large enough that the model trajectory falls within their range throughout roughly three-quarters of the path. Nonetheless, during the ball's descent, the model trajectory falls well outside of these bars. Most glaring about this inconsistency is the significant difference between the distances that the ball and the model each travel. Compared to the model, the ball travels nearly 0.2 m further—far greater a length than any uncertainties we have. This perhaps suggests an error in the formulation of the ball's initial velocity. In fact, the trajectory of a model with a slightly greater horizontal velocity, multiplied by a factor of 1.05(1), and slightly lower vertical velocity, multiplied by 0.96(1) more closely approximates that of the ball, as in Fig. 4. These adjustments are small enough that they may be attributable

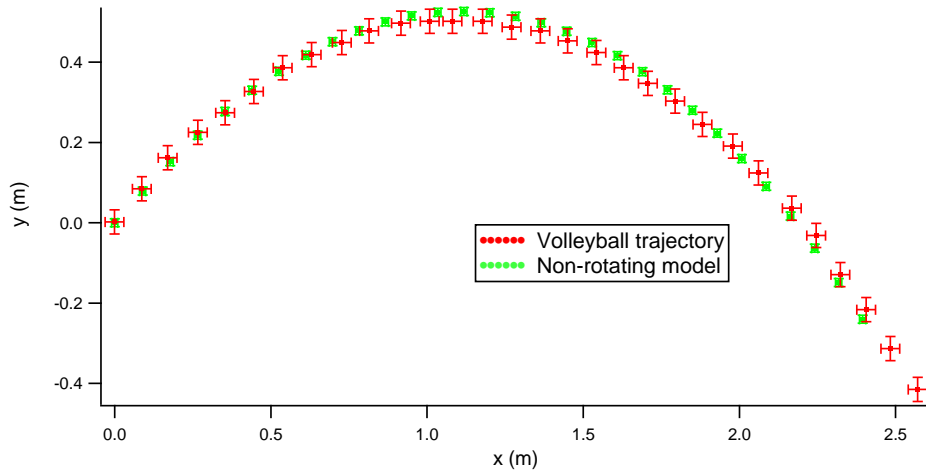


FIG. 3. The non-rotating volleyball's trajectory can be fit to our non-rotating model with a drag coefficient, b , of 0.01 kg/m . The ball travels in the positive x -direction beginning at $x=0$. As in the snapshot of Tracker, the red markers represent the ball's path, and the green, the model's. The error bars associated with the former arise from the inaccuracies inherent in picking out the trajectory of the ball in the software. The error bars on the model's markers arise, however, from uncertainties in the measurements of the constants and initial conditions used to create the model.

to unaccounted-for uncertainties in marking the position of the ball in the first two frames of our video, from which the program determines its initial velocity. However, the error could also be in the formulation of the model. Either way, more time to perform the same experiment would perhaps provide insight into this discrepancy.

Still, with a reasonable experimentally determined b -value in hand, we can shoot and analyze a video of an in-flight volleyball with topspin to see what effect its rotation has on its trajectory. We update our model to include a Magnus force and optimize C_ℓ in order to fit the new trajectory of the ball, once again selecting the model path that follows the ball's for the most time. We test lift coefficients ranging from 0 to 0.3. A C_ℓ of 0 corresponds to no Magnus effect, while 0.2 is roughly the value for the lift coefficient of a soccer ball corroborated by others, including Daish, de Mestre, Mehta and Pallis.⁵⁻⁷ Considering their nearly equal sizes, we expect the coefficients for soccer balls and volleyballs to be similar. Indeed, Mehta and Pallis consider the aerodynamics of volleyballs and soccer balls to be closely related, too.⁷ Somewhat in agreement with these findings, Fig. 5 shows that a lift coefficient of $0.25(2)$

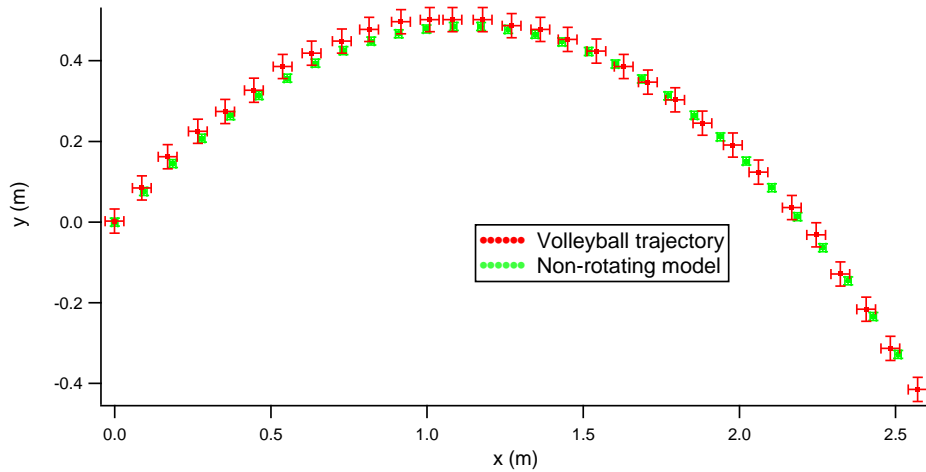


FIG. 4. The non-rotating ball's trajectory can be fit more closely with a model that uses slightly modified initial velocities. Increasing the model's horizontal velocity by a factor of 0.05 and decreasing its vertical velocity by a factor of 0.04 roughly halves the difference in the distances traveled by the ball and the model. As in Fig. 2, the red path is the ball's and the green path is the model's. The drag coefficient and error bars are the same.

most closely fits Eqs. 9 and 10 to the motion of our rotating volleyball. This is despite the fact that the experimental data listed in Bray and Kerwin, from which they calculated the lift coefficient of a soccer ball, involves ball velocities no less than 23 m/s, far greater the maximum velocity of ≈ 6.5 m/s we consider. This suggests that, at least in the region of velocities we consider, there is little correlation between the velocity of the ball and its lift coefficient.

Still, our model's path does not follow that of the rotating volleyball throughout its entire trajectory for any lift coefficient. Near the apex of the ball's flight, the difference between our model and the ball exceeds our propagated uncertainties. Similar to the procedure in the non-rotating experiment, we can obtain a better approximation of the ball's trajectory with our model if we increase its initial velocity in the horizontal direction and decrease it in the vertical direction. However, these adjustments are much greater than the ones shown in Fig. 4 and suggest that perhaps something other than our inaccurate selection of the ball's initial position is affecting the flight path.

To address this problem, we could attempt to perform our experiments again with higher velocities, closer to the range considered in Daish and de Mestre, among others. We could also find past experiments with launch velocities more similar to ours, in the hopes that their discussions of the rel-

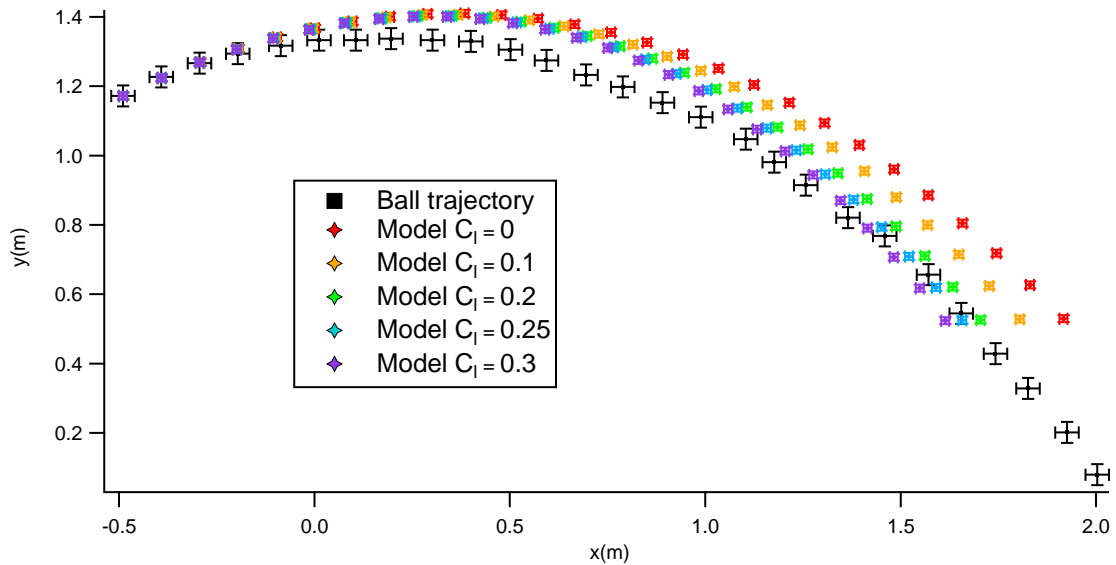


FIG. 5. The rotating volleyball's path through the air cannot be completely fit with our model incorporating gravity, quadratic drag, and Magnus effects. The black trajectory represents that of the ball, whereas the others correspond to the various models we tried, each with a different lift coefficient. As in Fig. 3, the error bars associated with the ball's path arise from the inaccuracies inherent in picking out the trajectory of the ball through Tracker, but the error bars on the models' trajectories result from uncertainties in the measurements of the constants and initial conditions used to create the models.

evant forces acting on the ball allow us to improve our models, whether by altering the equations for forces we already consider or introducing new ones. Additionally, a more consistent launching device—a machine, instead of our hands—would allow us to repeat the experiment and compare results across the various trials. Multiple trials would especially help to suppress errors in ascertaining the ball's initial velocity.

Finally, the ability to directly measure the direction of the ball's spin axis, whether by drawing on the ball or by some other method, requires further investigation. If we could discern the actual direction of $\hat{\omega} \times \hat{v}$ in our calculation of the Magnus effect, we could test the validity of our assumption that we can separate the effects of topspin into horizontal and vertical components as we

did.

* Corresponding author.

¹ Ken Bray and David G. Kerwin. Modelling the flight of a soccer ball in a direct free kick. *Journal of Sports Sciences*, 2003.

² Douglas Brown. Tracker. <http://www.cabrillo.edu/~dbrown/tracker/>, 2013.

³ Glenn Research Center. What is Lift? <http://www.grc.nasa.gov/www/k-12/airplane/lift1.html>, 2010.

⁴ Glenn Research Center. The Drag Coefficient. <http://www.grc.nasa.gov/www/k-12/airplane/dragco.html>, 2010.

⁵ C.B. Daish. *The Physics of Ball Games*. English Universities Press, 1972.

⁶ Neville de Mestre. *The Mathematics of Projectiles in Sport*. Cambridge University Press, 1990.

⁷ Rabindra D. Mehta and Jani Macari Pallis. Sports ball aerodynamics: Effects of velocity, spin and surface roughness. *Materials and Science in Sports*, 2001.

⁸ John R. Taylor. *Classical Mechanics*. University Science Books, 2005.

⁹ D.J. Tritton. *Physical Fluid Dynamics, 2nd ed.* Oxford University Press, 1988, 93.